Nonlinear Analysis: Modelling and Control, Vol. 31, No. 1, 45–67
https://doi.org/10.15388/namc.2026.31.44128

Vilnius University Press

# Quantization-based event-triggered control for synchronization of 2-D discrete-time switched master-slave systems in Roesser model*

**Zhimin Zhou, Lei Shi[1], Wenbo Liu, Xilong Luo, Shiqi Mo, Jiayin Mou**

School of Mathematics and Statistics,
Guilin University of Technology,
Guilin 541004, China

13873454439@163.com; shileilk@163.com;
19937148746@163.com; 13712508418@163.com;
15777391521@163.com; mu61276376@163.com

**Received:** March 24, 2025 / **Revised:** August 13, 2025 / **Published online:** January 1, 2026

**Abstract.** This paper investigates synchronization control for 2-D discrete-time switched master-slave systems modeled by the Roesser framework, which is classic for spatiotemporal dynamics in 2-D systems. A novel quantization-based event-triggered control strategy is proposed to handle complexities from switching dynamics, discrete-time features, and spatial coupling, while considering limited communication resources. By designing a mode-dependent event-triggered strategy and constructing mode-dependent Lyapunov functions for horizontal and vertical dynamics, new sufficient conditions are derived to ensure global exponential synchronization (GES) of the system. The approach relaxes strict stability requirements for individual modes, allowing global stability even with unstable modes. Additionally, the integration of quantization techniques and event-triggered mechanisms significantly reduces data transmission, thereby optimizing network bandwidth usage. Numerical simulations verify the method's effectiveness.

**Keywords:** 2-D switched systems, event-triggered control, quantization, synchronization, stability.

## 1 Introduction

In the era of rapid advancements in intelligent control and computational engineering, discrete-time systems have emerged as a cornerstone for modeling dynamic processes, with two-dimensional (2-D) discrete-time switched systems have attracted significant attention due to their distinctive structural properties and versatile synchronization capabilities. These systems play a pivotal role in addressing the synchronization challenges prevalent across interdisciplinary domains, including neural networks [1, 13], multiagent

*Jointly supported by the natural science foundation of Guangxi (No. 2022GXNSFAA035584).
[1]Corresponding author.

systems [2, 6, 8], and avionics [18, 21], where spatiotemporal coordination and mode-dependent dynamics are critical for system performance.

In neural network [10, 17], 2-D discrete-time switched models serve as effective tools for describing hierarchical spatiotemporal dependencies, enabling the synchronization of distributed state evolutions across both temporal sequences and spatial layers. This is particularly essential for capturing complex pattern correlations in sequential/spatial data such as the frame-wise feature consistency in image sequences or the layer-wise activation synchronization in deep neural networks. In multiagent systems [3, 7], the discrete-time framework of switched dynamics provides a rigorous foundation for designing synchronization protocols that facilitate coordinated collective behaviors. By integrating switching mechanisms, these systems can achieve robust consensus under heterogeneous communication topologies, ensuring coherent state alignment and optimal resource allocation among agents. The avionics field further benefits from the synchronization-oriented design of 2-D discrete-time switched systems, where real-time coordination of subsystem dynamics is imperative for fault-tolerant control and adaptive navigation. During flight condition transitions or component failures, these systems enable seamless synchronization between multisensor spatiotemporal measurements and adaptive control modes, ensuring stable trajectory tracking and reliable system reconfiguration. Ultimately, the intrinsic ability of 2-D discrete-time switched systems to model both spatial-temporal dynamics and mode-dependent switching behaviors renders them indispensable for addressing the synchronization complexities in high-dimensional distributed systems. Their applications highlight the critical role of systematic synchronization analysis in enabling reliable operation across diverse engineering scenarios, thereby motivating the exploration of novel theoretical frameworks for enhancing synchronization performance in such systems.

The analysis of synchronization problems in 2-D discrete-time switched systems presents significantly greater complexity than that of traditional 1-D discrete-time systems. This heightened complexity manifests primarily in three key aspects. These systems comprise multiple distinct subsystems that activate at different times through switching signals. The potentially heterogeneous dynamic characteristics across these subsystems, coupled with discontinuities induced by the switching process itself, can lead to instability and render the system behavior difficult to capture using a single unified model. For instance, switching between sensor data fusion rules in avionics systems during different flight modes may induce abrupt state variations, thereby degrading synchronization performance. As discrete-time systems update their states and control inputs solely at sampling instants, the selection of an appropriate sampling period becomes critical. An excessively long period inevitably introduces state tracking lag, while an overly short period imposes excessive computational and communication burdens. This trade-off is evident in applications like multiagent formation control, where frequent sampling can exacerbate network congestion, whereas sparse sampling might precipitate coordination failure. The intricate coupling between the system's 2-D state variables – involving complex interactions such as those between horizontal and vertical dynamics – further complicates the design of synchronization controllers. Consequently, control methodologies effective for 1-D discrete-time systems often cannot be directly generalized to their 2-D

counterparts under switching scenarios. Driven by the above mentioned complexities, a thorough investigation into the synchronization problems of 2-D discrete-time switched systems is hereby undertaken, which constitutes one of the research motivations of this paper.

Although the research on the synchronization of 2-D discrete-time systems is relatively limited compared to that of 1-D discrete-time systems, there are still few notable works regarding the synchronization of 2-D discrete systems. For example, in [12], Liang investigated the robust synchronization problem for 2-D discrete-time coupled dynamic networks. Their work utilized the Fornasini–Marchesini model to establish a nonlinear state-space representation and introduced a novel synchronization concept characterized by decoupled network dynamics and coupling across both spatial dimensions. However, their formulation did not explicitly account for constraints on sampling frequency or communication resource utilization. This oversight raises concerns regarding persistent resource consumption during system operation, potentially leading to an unsustainable communication burden in practical implementations with limited bandwidth or energy resources. In [15], Qin investigated the synchronization problem of discrete-time switched 2-D systems under Markov topology. The designed state feedback output controller requires continuous sampling of the system output, which overlooks the scenario of limited resources in practical applications, thus leading to limitations in its engineering implementation. In [22], Yang's research addresses the event-triggered control problem for discrete-time 2-D switched FM systems, introducing an event-triggered mechanism to efficiently utilize limited communication resources. However, the study implicitly assumes that all subsystems maintain stability, a premise that deviates from practical application requirements where subsystem stability cannot be universally guaranteed. Moreover, existing investigations into system control and associated methodologies have predominantly centered on 1-D discrete-time systems. Notable examples include sliding mode control [4, 25], predictive control [16, 26], and adaptive control [5, 19], which have undergone extensive exploration in this domain. In sharp contrast, published research integrating these control approaches with 2-D discrete-time system control remains remarkably limited. Additionally, the time-triggered strategies employed in certain prior studies give rise to suboptimal utilization of network bandwidth and communication resources. Thus, the dual objectives of filling the research gaps in 2-D systems and addressing the aforementioned shortcomings in existing findings serve as the key driving forces behind this study.

Event-triggered control (ETC) strategies [20, 23] have emerged as innovative and effective solutions to address the aforementioned challenges. By using event triggering, the control signals of a system are only updated and transmitted when the system states satisfy pre-defined triggering conditions. This strategy significantly reduces unnecessary communication overhead and conserves network bandwidth, making it particularly suitable for resource-constrained systems. It enables dynamic response to environmental changes and avoids meaningless periodic sampling, thus reducing resource consumption. Quantization techniques [24] represent another efficient approach to tackle these issues, which have been widely adopted in various systems. By discretizing continuous signal values into a finite set of quantization levels, they substantially alleviate the burden on network bandwidth. This not only enhances the efficiency of data transmission

but also ensures compatibility with systems operating under limited computational and communication resources. The integration of ETC and quantization techniques [9, 14] has become a promising approach to solve the synchronization problem in discrete-time systems. Specifically, applying this combined method to the synchronization control of 2-D discrete-time switched systems holds significant theoretical and practical implications. This approach not only facilitates the design of robust and efficient control strategies but also overcomes the limitations of traditional control methods, which often suffer from excessive communication costs and computational burdens. Furthermore, this framework can be extended to various real-world systems, including networked control systems and distributed systems, where efficient and reliable control solutions are of paramount importance.

Overall, to achieve synchronization in 2-D discrete-time switched systems described by the Roesser model, this paper proposes a mode-dependent event-triggered strategy integrated with quantization technique, where triggering intervals can be flexibly adjusted by tuning event-triggered parameters. To ensure GES, mode-dependent Lyapunov functions are independently constructed for horizontal and vertical dynamics, enabling the derivation of a series of new sufficient conditions to guarantee effective system synchronization. These conditions relax the strict requirements on the stability of certain modes imposed in previous studies, thereby enhancing the flexibility and applicability of the control strategy.

The principal contributions of this paper are highlighted as follows:

(i) This paper first investigates event-triggered synchronization control for 2-D discrete-time switched Roesser systems, where stability constraints on individual modes are relaxed to guarantee global stability even in the presence of unstable modes.

(ii) A mode-dependent event-triggered control strategy is proposed, establishing new sufficient conditions for GES via mode-dependent Lyapunov functions designed for horizontal and vertical dynamics, combined with stochastic switching analysis.

(iii) A quantization-based event-triggered controller is designed to reduce bandwidth consumption and optimize data transmission efficiency. Designed triggering conditions ensure control performance without degradation, making it suitable for network-constrained scenarios.

The subsequent sections are organized as follows: Section 2 designs a novel mode-dependent event-triggered control strategy. Section 3 presents a theoretical analysis of the system's GES. Section 4 provides a numerical example to validate the proposed controller's effectiveness. Section 5 summarizes the research findings.

**Notations.** $\mathbb{R}^n$ denotes the $n$-dimensional Euclidean vector space, and $\mathbb{R}^{n\times m}$ represents the set of all matrices of size $n \times m$. $\|\cdot\|$ is the Euclidean norm of vectors and matrices. $A^{\mathrm{T}}$ denotes the transpose of matrix $A$, and $A^{-1}$ denotes the inverse of $A$. $\mathrm{sym}\{A\}$ stands for $A + A^{\mathrm{T}}$. $A > 0$ ($A < 0$) signifies that matrix $A$ is positive (negative) definite. The identity matrix of dimension $n \times n$ is represented by $I_n$, while the zero matrix of

dimensions $m \times n$ is denoted by $0_{m\times n}$. $\lambda_{\max}(A)$ denotes the maximum eigenvalue of a real matrix $A$. $\mathbf{E}[\cdot]$ denotes the mathematical expectation of a random variable. The set $\mathbb{N}$ represents the set of nonnegative integers.

## 2 Preliminaries

Consider the following class of 2-D discrete-time switched master-slave systems described by the Roesser model:

- the master system

$$\begin{aligned}\begin{bmatrix}x^{\mathrm{h}}(i+1,\,j)\\ x^{\mathrm{v}}(i,\,j+1)\end{bmatrix} &= \begin{bmatrix}A_{11}^{\alpha(i,j)} & A_{12}^{\alpha(i,j)}\\ A_{21}^{\alpha(i,j)} & A_{22}^{\alpha(i,j)}\end{bmatrix}\begin{bmatrix}x^{\mathrm{h}}(i,j)\\ x^{\mathrm{v}}(i,j)\end{bmatrix},\\ y(i,j) &= \begin{bmatrix}C_1^{\alpha(i,j)} & C_2^{\alpha(i,j)}\end{bmatrix}\begin{bmatrix}x^{\mathrm{h}}(i,j)\\ x^{\mathrm{v}}(i,j)\end{bmatrix},\end{aligned} \tag{1}$$

- the slave system

$$\begin{aligned}\begin{bmatrix}\widetilde{x}^{\mathrm{h}}(i+1,\,j)\\ \widetilde{x}^{\mathrm{v}}(i,\,j+1)\end{bmatrix} &= \begin{bmatrix}A_{11}^{\alpha(i,j)} & A_{12}^{\alpha(i,j)}\\ A_{21}^{\alpha(i,j)} & A_{22}^{\alpha(i,j)}\end{bmatrix}\begin{bmatrix}\widetilde{x}^{\mathrm{h}}(i,j)\\ \widetilde{x}^{\mathrm{v}}(i,j)\end{bmatrix} + \begin{bmatrix}B_1^{\alpha(i,j)}\\ B_2^{\alpha(i,j)}\end{bmatrix}u(i,j),\\ \widetilde{y}(i,j) &= \begin{bmatrix}C_1^{\alpha(i,j)} & C_2^{\alpha(i,j)}\end{bmatrix}\begin{bmatrix}\widetilde{x}^{\mathrm{h}}(i,j)\\ \widetilde{x}^{\mathrm{v}}(i,j)\end{bmatrix},\end{aligned} \tag{2}$$

- the error system

$$\begin{aligned}\begin{bmatrix}e^{\mathrm{h}}(i+1,\,j)\\ e^{\mathrm{v}}(i,\,j+1)\end{bmatrix} &= \begin{bmatrix}A_{11}^{\alpha(i,j)} & A_{12}^{\alpha(i,j)}\\ A_{21}^{\alpha(i,j)} & A_{22}^{\alpha(i,j)}\end{bmatrix}\begin{bmatrix}e^{\mathrm{h}}(i,j)\\ e^{\mathrm{v}}(i,j)\end{bmatrix} + \begin{bmatrix}B_1^{\alpha(i,j)}\\ B_2^{\alpha(i,j)}\end{bmatrix}u(i,j),\\ z(i,j) &= \begin{bmatrix}C_1^{\alpha(i,j)} & C_2^{\alpha(i,j)}\end{bmatrix}\begin{bmatrix}e^{\mathrm{h}}(i,j)\\ e^{\mathrm{v}}(i,j)\end{bmatrix},\end{aligned} \tag{3}$$

where $x^{\mathrm{h}}(i,j) \in \mathbb{R}^{n_{\mathrm{h}}}$, $\widetilde{x}^{\mathrm{h}}(i,j) \in \mathbb{R}^{n_{\mathrm{h}}}$, and $e^{\mathrm{h}}(i,j) \in \mathbb{R}^{n_{\mathrm{h}}}$ represent the horizontal state vectors of the corresponding systems. $x^{\mathrm{v}}(i,j) \in \mathbb{R}^{n_{\mathrm{v}}}$, $\widetilde{x}^{\mathrm{v}}(i,j) \in \mathbb{R}^{n_{\mathrm{v}}}$, and $e^{\mathrm{v}}(i,j) \in \mathbb{R}^{n_{\mathrm{v}}}$ represent the vertical state vectors of the corresponding systems. $y(i,j) \in \mathbb{R}^{n_l}$, $\widetilde{y}(i,j) \in \mathbb{R}^{n_l}$, and $z(i,j) \in \mathbb{R}^{n_l}$ represent the output vectors of the corresponding systems. $u(i,j) \in \mathbb{R}^m$ is the control input of the system. $\alpha(i,j)$ represents the switching signal of controller, where $\alpha(i,j) : \mathbb{N} \times \mathbb{N} \to M = \{1,2,\ldots,N\}$ with $N$ being the number of modes in the system. $A_{11}^{\alpha(i,j)} \in \mathbb{R}^{n_{\mathrm{h}}\times n_{\mathrm{h}}}$, $A_{12}^{\alpha(i,j)} \in \mathbb{R}^{n_{\mathrm{h}}\times n_{\mathrm{v}}}$, $A_{21}^{\alpha(i,j)} \in \mathbb{R}^{n_{\mathrm{v}}\times n_{\mathrm{h}}}$, $A_{22}^{\alpha(i,j)} \in \mathbb{R}^{n_{\mathrm{v}}\times n_{\mathrm{v}}}$, $B_1^{\alpha(i,j)} \in \mathbb{R}^{n_{\mathrm{h}}\times m}$, $B_2^{\alpha(i,j)} \in \mathbb{R}^{n_{\mathrm{v}}\times m}$, $C_1^{\alpha(i,j)} \in \mathbb{R}^{n_l\times n_{\mathrm{h}}}$, and $C_2^{\alpha(i,j)} \in \mathbb{R}^{n_l\times n_{\mathrm{v}}}$ are known real matrices.

The boundary conditions for systems (1), (2), and (3) are formulated as follows:

$$\begin{aligned}x_0 &= \big\{x^{\mathrm{h}}(0,j), x^{\mathrm{v}}(i,0) \;\big|\; i,j \in \mathbb{N}\big\},\\ \widetilde{x}_0 &= \big\{\widetilde{x}^{\mathrm{h}}(0,j), \widetilde{x}^{\mathrm{v}}(i,0) \;\big|\; i,j \in \mathbb{N}\big\},\\ e_0 &= \big\{e^{\mathrm{h}}(0,j), e^{\mathrm{v}}(i,0) \;\big|\; i,j \in \mathbb{N}\big\}.\end{aligned}$$

We generally consider that the aforementioned boundary conditions are bounded and $e_0$ satisfies the following criteria:

$$\limsup_{T\to\infty} \mathbf{E}\left\{ \sum_{t=0}^{\mathrm{T}} \left( \left\| e^{\mathrm{h}}(0,t) \right\|^2 + \left\| e^{\mathrm{v}}(t,0) \right\|^2 \right) \right\} < \infty.$$

Notably, it is crucial to underscore that investigating the synchronization control problem between the master system (1) and the slave system (2) is fundamentally equivalent to studying the error system (3). Consequently, the primary emphasis of subsequent analyses will be placed on the error system (3).

**Assumption 1.** The switching behavior of system (3) is postulated to depend exclusively on two independent variables $i$ and $j$ evolving along distinct directions. Specifically, the switching signal $\alpha(i,j)$ is determined uniquely by $i+j$. For any $t \in \mathbb{N}$, whenever $i+j=t$, the switching signal takes the form

$$\alpha(i,j) = \alpha(t) = r, \quad r \in M.$$

In system (3), the switching occurs randomly. According to Assumption 1, each system shall comply with the following stochastic switching rules.

**Definition 1.** For any $\varphi, \psi \in M$, the switching signal $\alpha(t)$ shifts from the mode corresponding to index $\varphi$ to the mode corresponding to index $\psi$, based on the system's transition probability matrix (TPM). Specifically, this transition is governed by the following probability:

$$\mathbf{P}\big\{\alpha(t+1) = \psi \mid \alpha(t) = \varphi\big\} = \kappa_{\varphi\psi},$$

where $\kappa_{\varphi\psi}$ represents the TPM from mode $\varphi$ to mode $\psi$.

When $\varphi = \psi$, we have $\kappa_{\varphi\psi} = 0$, whereas when $\varphi \neq \psi$, the transition probabilities satisfy $0 \leqslant \kappa_{\varphi\psi} < 1$ with the additional constraint that

$$\sum_{\psi=1}^{N} \kappa_{\varphi\psi} = 1.$$

The TPM is an irreducible matrix, implying the existence of a unique stationary distribution $\epsilon = (\epsilon_1, \epsilon_2, \ldots, \epsilon_N)$ with $\sum_{l=1}^{N} \epsilon_l = 1$. Under Assumption 1, for any time interval $t \in [t_{s-1}, t_s)$, the sequence of mode switching times for system (3), given by $\{t_s = i_s + j_s,\ s \in \mathbb{N}\}$, must satisfy

$$0 = t_0 < t_1 < \cdots < t_s < \cdots$$

and

$$\lim_{s\to+\infty} t_s = +\infty.$$

The dwell time, defined as the duration spent in a particular mode before switching to another, is denoted as

$$d^r(s) = t_s - t_{s-1} < +\infty.$$

**Assumption 2.** The expected dwell time in mode $r$ is defined as

$$\mathbf{E}\big[d^r(s)\big] = \gamma^r, \quad r \in M,$$

where $\gamma^r$ represents the mean dwell time for mode $r$, and it satisfies $\gamma^r > 0$.

**Definition 2.** Provided that the following condition holds, system (3) achieves the GES:

$$\limsup_{t\to\infty} \frac{\ln(\sum_{t=i+j} \|e(i,j)\|)}{t} < 0$$

with

$$e(i,j) = \begin{bmatrix} e^{\mathrm{h}}(i+1,\, j) \\ e^{\mathrm{v}}(i,\, j+1) \end{bmatrix}.$$

Next, we will present the mode-dependent event-triggered conditions. When $\alpha(i,j) = \alpha(t) = r$ for $t \in [t_s, t_{s+1})$, we define $t_s^\tau = i_s^\tau + j_s^\tau$ and $t_s = i_s + j_s$ with $s \in \mathbb{N}$. Here $\tau \in \mathbb{N}$ represent the $\tau$th sampling instant within the specified time interval. The sampling instants $t_s^\tau$ are chosen so that they fulfill the following criterion:

$$t_s = t_s^0 < t_s^1 < \cdots < t_{s+1}.$$

It is important to note that $t_s = t_s^0$ signifies both the initial sampling instant and the onset of the $r$th mode within the interval $[t_s, t_{s+1})$. Hence, the timing of the system sampling instants $t_s^\tau$ is strictly influenced by the system's switching signal $\alpha(t)$. The construction of a mode-dependent event-triggered strategy for system (3) is provided by

$$t_s^{\tau+1} = \min\left\{ t > t_s^\tau \;\middle|\; \vartheta(i,j)^{\mathrm{T}} \Theta^r \vartheta(i,j) > \xi^r z\big(i_s^\tau, j_s^\tau\big)^{\mathrm{T}} \Theta^r z\big(i_s^\tau, j_s^\tau\big) + \frac{1}{2}\gamma\delta^{\lambda t} \right\}, \quad (4)$$

where $\vartheta(i,j) = z(i_s^\tau, j_s^\tau) - z(i,j)$ with $0 < \Theta^r \in \mathbb{R}^{n_l \times n_l}$, $r \in M$. Additionally, the scalar parameters are constrained as follows: $\lambda > 1$, $\gamma > 0$, $0 < \delta < 1$, and $0 < \xi^r < 1$.

**Remark 1.** Research on synchronization of 2-D discrete-time switched systems remains limited. For example, [15] proposed an output feedback control for 2-D discrete-time switched FM systems, but its controller demands frequent sampling, failing to reduce data transmission. This paper focuses on synchronization of 2-D discrete-time switched systems under the Roesser model. Considering their substantial data transmission requirements, a novel event-triggered control strategy with quantization is introduced to address synchronization, which alleviates transmission burden while ensuring efficient performance.

**Remark 2.** The next sampling instant in (4) depends on parameters $\xi^r$, $\gamma$, and $\lambda$, whose combination can be flexibly selected per task requirements to adjust sampling intervals. Compared with the single-parameter adjustment method in [11], this strategy enhances flexibility and adaptability, enabling more efficient use of network resources while enriching system design diversity and practicality.

Following this, we describe the approach for designing the quantization-based event-triggered dynamic output controller:

$$\begin{aligned}\begin{bmatrix}\hat{e}^{\mathrm{h}}(i+1,\,j)\\ \hat{e}^{\mathrm{v}}(i,\,j+1)\end{bmatrix} &= \begin{bmatrix}\hat{A}_{11}^{\alpha(i,j)} & \hat{A}_{12}^{\alpha(i,j)}\\ \hat{A}_{21}^{\alpha(i,j)} & \hat{A}_{22}^{\alpha(i,j)}\end{bmatrix}\begin{bmatrix}\hat{e}^{\mathrm{h}}(i,j)\\ \hat{e}^{\mathrm{v}}(i,j)\end{bmatrix} + \begin{bmatrix}\hat{B}_{1}^{\alpha(i,j)}\\ \hat{B}_{2}^{\alpha(i,j)}\end{bmatrix} z\big(i_s^{\tau}, j_s^{\tau}\big),\\ h(i,j) &= \begin{bmatrix}\hat{C}_{1}^{\alpha(i,j)} & \hat{C}_{2}^{\alpha(i,j)}\end{bmatrix}\begin{bmatrix}\hat{e}^{\mathrm{h}}(i,j)\\ \hat{e}^{\mathrm{v}}(i,j)\end{bmatrix},\\ u(i,j) &= q\big(h(i,j)\big),\end{aligned} \tag{5}$$

where $\hat{e}^{\mathrm{h}}(i,j) \in \mathbb{R}^{n_{\hat{h}}}$ ($n_{\hat{h}} \leqslant n_{\mathrm{h}}$) and $\hat{e}^{\mathrm{v}}(i,j) \in \mathbb{R}^{n_{\hat{v}}}$ ($n_{\hat{v}} \leqslant n_{\mathrm{v}}$) are the horizontal and vertical state vectors of the controller, respectively; $\hat{A}_{11}^{\alpha(i,j)} \in \mathbb{R}^{n_{\hat{h}}\times n_{\hat{h}}}$, $\hat{A}_{12}^{\alpha(i,j)} \in \mathbb{R}^{n_{\hat{h}}\times n_{\hat{v}}}$, $\hat{A}_{21}^{\alpha(i,j)} \in \mathbb{R}^{n_{\hat{v}}\times n_{\hat{h}}}$, $\hat{A}_{22}^{\alpha(i,j)} \in \mathbb{R}^{n_{\hat{v}}\times n_{\hat{v}}}$, $\hat{B}_{1}^{\alpha(i,j)} \in \mathbb{R}^{n_{\hat{h}}\times n_{l}}$, $\hat{B}_{2}^{\alpha(i,j)} \in \mathbb{R}^{n_{\hat{v}}\times n_{l}}$, $\hat{C}_{1}^{\alpha(i,j)} \in \mathbb{R}^{m\times n_{\hat{h}}}$, and $\hat{C}_{2}^{\alpha(i,j)} \in \mathbb{R}^{m\times n_{\hat{v}}}$ are the control gain matrices; $t_s^{\tau} = i_s^{\tau} + j_s^{\tau}$ denotes the event-triggered instant; $h(i,j) = (h_1^{\mathrm{T}}(i,j),\, h_2^{\mathrm{T}}(i,j), \ldots, h_k^{\mathrm{T}}(i,j))^{\mathrm{T}}$ is the output, $g(i,j)$ represents a class of output vector, and $q(h(i,j)) = (q_1^{\mathrm{T}}(h_1(i,j)),\, q_2^{\mathrm{T}}(h_2(i,j)), \ldots, q_k^{\mathrm{T}}(h_k(i,j)))^{\mathrm{T}}$ is the quantizer. The quantizer satisfies $q_{\varrho}(\cdot) : \mathbb{R} \to U_{\varrho}$, where $\varrho = 1, 2, \ldots, k$, $U = \{\pm o_{\iota}\colon\ w_{\iota} = \varsigma_{\iota},\ 0 < \varsigma_{\iota} < 1,\ \iota \in \mathbb{Z}\} \cup \{0\}$, $\bar{o}_0 > 0$. For any $x \in \mathbb{R}$, the quantizer $q_{\varrho}(x)$ is defined as follows:

$$q_{\varrho}(x) = \begin{cases} o_{\iota} & \text{if } \frac{1}{1+\rho_{\varrho}}\bar{o}_i < x \leqslant \frac{1}{1-\rho_{\varrho}}\bar{o}_i,\ \rho_{\varrho} = \frac{1-\varsigma_{\varrho}}{1+\varsigma_{\varrho}},\\ 0 & \text{if } x = 0,\\ -q_{\varrho}(-x) & \text{if } x < 0,\end{cases}$$

By analyzing system (3) and controller (5), the following relationships can be derived:

1. The output state vector of the system in (3) is transmitted to the controller in (5) via the error output vector $z(i,j)$.
2. The controller in (5) computes control input vector $u(i,j)$ via error system state output vector $z(i,j)$from (3), then applies $u(i,j)$ to (3), thus implementing state feedback control based on the latter's dynamic output.

**Remark 3.** Controller (5) integrates event-triggered dynamic output control with quantization, effectively reducing network bandwidth consumption. Building on and optimizing the strategy in [15], it improves resource utilization and overall system performance for more efficient use of limited network resources, suiting applications with constrained networks yet demanding efficient dynamic control.

Similar to error system (3), the boundary conditions of controller (5) are ultimately bounded. It is demonstrated that the quantizer $q_{\varrho}(x)$ possesses Filippov solution $\omega^{\alpha(i,j)} \in [-\vartheta^{\alpha(i,j)}, \vartheta^{\alpha(i,j)}]$, in such a way that the quantizer takes the form of $q_{\varrho}(x) = (1 + \omega^{\alpha(i,j)})x$. Consequently, we derive the new controller as follows:

$$\begin{aligned}\begin{bmatrix}\hat{e}^{\mathrm{h}}(i+1,\,j)\\ \hat{e}^{\mathrm{v}}(i,\,j+1)\end{bmatrix} &= \begin{bmatrix}\hat{A}_{11}^{\alpha(i,j)} & \hat{A}_{12}^{\alpha(i,j)}\\ \hat{A}_{21}^{\alpha(i,j)} & \hat{A}_{22}^{\alpha(i,j)}\end{bmatrix}\begin{bmatrix}\hat{e}^{\mathrm{h}}(i,j)\\ \hat{e}^{\mathrm{v}}(i,j)\end{bmatrix} + \begin{bmatrix}\hat{B}_{1}^{\alpha(i,j)}\\ \hat{B}_{2}^{\alpha(i,j)}\end{bmatrix} z\big(i_s^{\tau}, j_s^{\tau}\big),\\ u(i,j) &= \big[I_m + \varpi^{\alpha(i,j)}\big]\begin{bmatrix}\hat{C}_{1}^{\alpha(i,j)} & \hat{C}_{2}^{\alpha(i,j)}\end{bmatrix}\begin{bmatrix}\hat{e}^{\mathrm{h}}(i,j)\\ \hat{e}^{\mathrm{v}}(i,j)\end{bmatrix}\end{aligned} \tag{6}$$

with $\varpi^{\alpha(i,j)} = \operatorname{diag}(\omega_1^{\alpha(i,j)}, \omega_2^{\alpha(i,j)}, \ldots, \omega_g^{\alpha(i,j)})$. By combining error system (3) and controller (6), the resulting augmented system is formulated in the following manner:

$$\begin{aligned}
\begin{bmatrix} e^{\mathrm{h}}(i+1,\, j) \\ e^{\mathrm{v}}(i,\, j+1) \end{bmatrix} &= \begin{bmatrix} A_{11}^{\alpha(i,j)} & A_{12}^{\alpha(i,j)} \\ A_{21}^{\alpha(i,j)} & A_{22}^{\alpha(i,j)} \end{bmatrix} \begin{bmatrix} e^{\mathrm{h}}(i,j) \\ e^{\mathrm{v}}(i,j) \end{bmatrix} \\
&\quad + \begin{bmatrix} B_1^{\alpha(i,j)} \\ B_2^{\alpha(i,j)} \end{bmatrix} \left[ I_m + \varpi^{\alpha(i,j)} \right] \begin{bmatrix} \hat{C}_1^{\alpha(i,j)} & \hat{C}_2^{\alpha(i,j)} \end{bmatrix} \begin{bmatrix} \hat{e}^{\mathrm{h}}(i,j) \\ \hat{e}^{\mathrm{v}}(i,j) \end{bmatrix}, \\
\begin{bmatrix} \hat{e}^{\mathrm{h}}(i+1,\, j) \\ \hat{e}^{\mathrm{v}}(i,\, j+1) \end{bmatrix} &= \begin{bmatrix} \hat{A}_{11}^{\alpha(i,j)} & \hat{A}_{12}^{\alpha(i,j)} \\ \hat{A}_{21}^{\alpha(i,j)} & \hat{A}_{22}^{\alpha(i,j)} \end{bmatrix} \begin{bmatrix} \hat{e}^{\mathrm{h}}(i,j) \\ \hat{e}^{\mathrm{v}}(i,j) \end{bmatrix} \\
&\quad + \begin{bmatrix} \hat{B}_1^{\alpha(i,j)} \\ \hat{B}_2^{\alpha(i,j)} \end{bmatrix} \left[ \begin{bmatrix} C_1^{\alpha(i,j)} & C_2^{\alpha(i,j)} \end{bmatrix} \begin{bmatrix} e^{\mathrm{h}}(i,j) \\ e^{\mathrm{v}}(i,j) \end{bmatrix} + \vartheta(i,j) \right].
\end{aligned} \tag{7}$$

Let $\chi^{\mathrm{h}}(i,j) = (e^{\mathrm{h}\mathrm{T}}(i,j), \hat{e}^{\mathrm{h}\mathrm{T}}(i,j))^{\mathrm{T}}$, $\chi^{\mathrm{v}}(i,j) = (e^{\mathrm{v}\mathrm{T}}(i,j), \hat{e}^{\mathrm{v}\mathrm{T}}(i,j))^{\mathrm{T}}$, $\chi(i,j) = (\chi^{\mathrm{h}\mathrm{T}}(i,j), \chi^{\mathrm{v}\mathrm{T}}(i,j))^{\mathrm{T}}$, and $\chi^*(i,j) = (\chi^{\mathrm{h}\mathrm{T}}(i+1,\, j), \chi^{\mathrm{v}\mathrm{T}}(i,\, j+1))^{\mathrm{T}}$. Subsequently, we can reformulate the augmented system (7) as

$$\chi^*(i,j) = \begin{bmatrix} \mathcal{A}^{\alpha(i,j)} & \mathcal{B}^{\alpha(i,j)} \\ \mathcal{C}^{\alpha(i,j)} & \mathcal{D}^{\alpha(i,j)} \end{bmatrix} \chi(i,j) + \begin{bmatrix} \mathcal{E}^{\alpha(i,j)} \\ \mathcal{F}^{\alpha(i,j)} \end{bmatrix} \vartheta(i,j), \tag{8}$$

where

$$\begin{aligned}
\mathcal{A}^{\alpha(i,j)} &= \begin{pmatrix} A_{11}^{\alpha(i,j)} & B_1^{\alpha(i,j)}[I_m + \varpi^{\alpha(i,j)}]\hat{C}_1^{\alpha(i,j)} \\ \hat{B}_1^{\alpha(i,j)} C_1^{\alpha(i,j)} & \hat{A}_{11}^{\alpha(i,j)} \end{pmatrix}, \\
\mathcal{B}^{\alpha(i,j)} &= \begin{pmatrix} A_{12}^{\alpha(i,j)} & B_1^{\alpha(i,j)}[I_m + \varpi^{\alpha(i,j)}]\hat{C}_2^{\alpha(i,j)} \\ \hat{B}_1^{\alpha(i,j)} C_2^{\alpha(i,j)} & \hat{A}_{12}^{\alpha(i,j)} \end{pmatrix}, \\
\mathcal{C}^{\alpha(i,j)} &= \begin{pmatrix} A_{21}^{\alpha(i,j)} & B_2^{\alpha(i,j)}[I_m + \varpi^{\alpha(i,j)}]\hat{C}_1^{\alpha(i,j)} \\ \hat{B}_2^{\alpha(i,j)} C_1^{\alpha(i,j)} & \hat{A}_{21}^{\alpha(i,j)} \end{pmatrix}, \\
\mathcal{D}^{\alpha(i,j)} &= \begin{pmatrix} A_{22}^{\alpha(i,j)} & B_2^{\alpha(i,j)}[I_m + \varpi^{\alpha(i,j)}]\hat{C}_2^{\alpha(i,j)} \\ \hat{B}_2^{\alpha(i,j)} C_2^{\alpha(i,j)} & \hat{A}_{22}^{\alpha(i,j)} \end{pmatrix}, \\
\mathcal{E}^{\alpha(i,j)} &= \begin{pmatrix} 0_{n_{\mathrm{h}} \times n_l} \\ \hat{B}_1^{\alpha(i,j)} \end{pmatrix}, \qquad \mathcal{F}^{\alpha(i,j)} = \begin{pmatrix} 0_{n_{\mathrm{v}} \times n_l} \\ \hat{B}_2^{\alpha(i,j)} \end{pmatrix}.
\end{aligned}$$

Let $\zeta(i,j) = (\chi^{\mathrm{h}\mathrm{T}}(i+1,\, j), \chi^{\mathrm{v}\mathrm{T}}(i,\, j+1), \chi^{\mathrm{h}\mathrm{T}}(i,j), \chi^{\mathrm{v}\mathrm{T}}(i,j), \vartheta^{\mathrm{T}}(i,j))^{\mathrm{T}}$. Hence, we derive the following result:

$$\begin{aligned}
\chi^{\mathrm{h}}(i+1,\, j) &= (I_a, 0_{a \times (a+2b+n_l)})\zeta(i,j) \triangleq E_1 \zeta(i,j), \\
\chi^{\mathrm{v}}(i,\, j+1) &= (0_{b \times a}, I_b, 0_{b \times (a+b+n_l)})\zeta(i,j) \triangleq E_2 \zeta(i,j),
\end{aligned}$$

$$\chi^{\mathrm{h}}(i,j) = (0_{a\times(a+b)}, I_a, 0_{a\times(b+n_l)})\zeta(i,j) \triangleq E_3\zeta(i,j),$$
$$\chi^{\mathrm{v}}(i,j) = (0_{b\times(2a+b)}, I_b, 0_{b\times n_l})\zeta(i,j) \triangleq E_4\zeta(i,j),$$
$$\vartheta(i,j) = (0_{n_l\times(2a+2b)}, I_{n_l})\zeta(i,j) \triangleq E_5\zeta(i,j),$$

and

$$z(i,j) = \begin{bmatrix} C_1^{\alpha(i,j)} & C_2^{\alpha(i,j)} \end{bmatrix} \begin{bmatrix} (0_{n_{\mathrm{h}}\times(a+b)}, I_{n_{\mathrm{h}}}, 0_{n_{\mathrm{h}}\times(n_{\hat{h}}+b+n_l)}) \\ (0_{n_{\mathrm{v}}\times(2a+b)}, I_{n_{\mathrm{v}}}, 0_{n_{\mathrm{v}}\times(n_{\hat{v}}+n_l)}) \end{bmatrix} \zeta(i,j)$$
$$\triangleq \big(C_1^{\alpha(i,j)}E_6 + C_2^{\alpha(i,j)}E_7\big)\zeta(i,j)$$

with $a = n_{\mathrm{h}} + n_{\hat{h}}$, $b = n_{\mathrm{v}} + n_{\hat{v}}$. Hence, (8) is transformed into

$$\chi^*(i,j) = \begin{bmatrix} E_1 \\ E_2 \end{bmatrix} \zeta(i,j)$$
$$= \begin{bmatrix} \mathcal{A}^{\alpha(i,j)} & \mathcal{B}^{\alpha(i,j)} \\ \mathcal{C}^{\alpha(i,j)} & \mathcal{D}^{\alpha(i,j)} \end{bmatrix} \begin{bmatrix} E_3 \\ E_4 \end{bmatrix} \zeta(i,j) + \begin{bmatrix} \mathcal{E}^{\alpha(i,j)} \\ \mathcal{F}^{\alpha(i,j)} \end{bmatrix} E_5\zeta(i,j). \tag{9}$$

Our objective is to achieve the GES of the 2-D discrete-time switched master-slave systems in Roesser model through the ETC condition (4) and the controller (5).

**Lemma 1.** (*See* [24].) *If $\alpha(i,j) = \alpha(t) = r$, where $t = i + j$, $r \in M$ represents the switching signal, and $\epsilon$ is the unique stationary distribution of the TPM associated with a mode-dependent average dwell time (ADT) technique, then we have*

$$\lim_{t\to\infty} \frac{T^r(t)}{t} = \bar{\epsilon}^r,$$

*where $\bar{\epsilon}^r = \epsilon^r\gamma^r/(\sum_{l=1}^N \epsilon^l\gamma^l)$, and $T^r(t)$ denotes the cumulative dwell time of the switching signal $\alpha(t) = r$ within the time interval $[0,t]$.*

## 3 Main results

In this section, we will discuss the GES of error system (3) under the influence of controller (5). In subsequent analyses, new techniques will be employed to design the Lyapunov function as a mode-dependent function for Theorem 1. Additionally, ergodic theory will be utilized to theoretically analyze the properties of the unique stationary distribution $\epsilon$. By resolving LMIs detailed in Theorem 2, one can determine the control gains for controller (5).

**Theorem 1.** *Under Assumptions* 1–2*, suppose that all control gain matrices $\hat{A}_{11}^r$, $\hat{A}_{12}^r$, $\hat{A}_{21}^r$, $\hat{A}_{22}^r$, $\hat{B}_1^r$, $\hat{B}_2^r$, $\hat{C}_1^r$, $\hat{C}_2^r$ are known. If for given scalars $\delta^r > 0$, $\beta^r \geqslant 1$, there exists matrices $0 < Q_r^{\mathrm{h}} \in \mathbb{R}^{(n_{\mathrm{h}}+n_{\hat{h}})\times(n_{\mathrm{h}}+n_{\hat{h}})}$, $0 < Q_r^{\mathrm{v}} \in \mathbb{R}^{(n_{\mathrm{v}}+n_{\hat{v}})\times(n_{\mathrm{v}}+n_{\hat{v}})}$, $0 < \Theta^r \in \mathbb{R}^{n_l\times n_l}$ and invertible matrices $U_1^r \in \mathbb{R}^{(n_{\mathrm{h}}+n_{\hat{h}})\times(n_{\mathrm{h}}+n_{\hat{h}})}$, $U_2^r \in \mathbb{R}^{(n_{\mathrm{v}}+n_{\hat{v}})\times(n_{\mathrm{v}}+n_{\hat{v}})}$,*

$W^r \in \mathbb{R}^{n_l \times n_l}$ *such that*

$$\Upsilon^r < 0, \tag{10}$$

$$Q_r^{\mathrm{h}} \leqslant \beta^r Q_{\tilde{r}}^{\mathrm{h}}, \quad Q_r^{\mathrm{v}} \leqslant \beta^r Q_{\tilde{r}}^{\mathrm{v}}, \quad r \neq \tilde{r} \text{ and } \tilde{r} \in M, \tag{11}$$

$$\sum_{r=1}^{N} \bar{\epsilon}^r \left[ \frac{\ln \beta^r}{\gamma^r} + \ln \delta^r \right] < 0,$$

*then, upon application of the controller specified in* (5)*, the error system described by* (3) *achieves the GES, where*

$$\Upsilon^r = \begin{pmatrix} \Upsilon_{11}^r & \Upsilon_{12}^r \\ * & \Pi^r \end{pmatrix}$$

*with*

$$\begin{aligned}
\Upsilon_{11}^r &= \operatorname{diag}\big(Q_r^{\mathrm{h}} - U_1^r - U_1^{r\mathrm{T}},\, Q_r^{\mathrm{v}} - U_2^r - U_2^{r\mathrm{T}},\, \xi^r \Theta^r - W^r - W^{r\mathrm{T}}\big), \\
\Upsilon_{12}^r &= \big(\big(U_1^r E_1\big)^{\mathrm{T}},\, \big(U_2^r E_2\big)^{\mathrm{T}},\, \big(W^r \big(C_1^r E_6 + C_2^r E_7 + E_5\big)\big)^{\mathrm{T}}\big)^{\mathrm{T}}, \\
\Pi^r &= \operatorname{sym}\big\{E_1^{\mathrm{T}} \mathcal{A}^r E_3 + E_1^{\mathrm{T}} \mathcal{B}^r E_4 + E_1^{\mathrm{T}} \mathcal{E}^r E_5 - E_1^{\mathrm{T}} E_1\big\} \\
&\quad + \operatorname{sym}\big\{E_2^{\mathrm{T}} \mathcal{C}^r E_3 + E_2^{\mathrm{T}} \mathcal{D}^r E_4 + E_2^{\mathrm{T}} \mathcal{F}^r E_5 - E_2^{\mathrm{T}} E_2\big\} \\
&\quad - \delta^r E_3^{\mathrm{T}} Q_r^{\mathrm{h}} E_3 - \delta^r E_4^{\mathrm{T}} Q_r^{\mathrm{v}} E_4 - \xi^r E_5^{\mathrm{T}} \Theta^r E_5.
\end{aligned}$$

*Proof.* When $\alpha(i,j) = \alpha(t) = r \in M$ (where $t = i + j \in [t_{s-1}, t_s)$), to analyze the synchronization issue for the error system (3), we propose the mode-dependent Lyapunov functions

$$\begin{aligned}
V_r\big(\chi(i,j)\big) &= V_r^{\mathrm{h}}\big(\chi^{\mathrm{h}}(i,j)\big) + V_r^{\mathrm{v}}\big(\chi^{\mathrm{v}}(i,j)\big), \\
V_r\big(\chi^*(i,j)\big) &= V_r^{\mathrm{h}}\big(\chi^{\mathrm{h}}(i+1,\, j)\big) + V_r^{\mathrm{v}}\big(\chi^{\mathrm{v}}(i,\, j+1)\big),
\end{aligned}$$

where

$$\begin{aligned}
V_r^{\mathrm{h}}\big(\chi^{\mathrm{h}}(i,j)\big) &= \chi^{\mathrm{h}\mathrm{T}}(i,j) Q_r^{\mathrm{h}} \chi^{\mathrm{h}}(i,j), \\
V_r^{\mathrm{v}}\big(\chi^{\mathrm{v}}(i,j)\big) &= \chi^{\mathrm{v}\mathrm{T}}(i,j) Q_r^{\mathrm{v}} \chi^{\mathrm{v}}(i,j), \\
V_r^{\mathrm{h}}\big(\chi^{\mathrm{h}}(i+1,\, j)\big) &= \chi^{\mathrm{h}\mathrm{T}}(i+1,\, j) Q_r^{\mathrm{h}} \chi^{\mathrm{h}}(i+1,\, j), \\
V_r^{\mathrm{v}}\big(\chi^{\mathrm{v}}(i,\, j+1)\big) &= \chi^{\mathrm{v}\mathrm{T}}(i,\, j+1) Q_r^{\mathrm{v}} \chi^{\mathrm{v}}(i,\, j+1).
\end{aligned}$$

To facilitate further analysis, we formulate the difference in the following structure:

$$\begin{aligned}
&\Delta V_r^{\mathrm{h}}\big(\chi^{\mathrm{h}}(i,j)\big) - \big(\delta^r - 1\big) V_r^{\mathrm{h}}\big(\chi^{\mathrm{h}}(i,j)\big) \\
&\quad = V_r^{\mathrm{h}}\big(\chi^{\mathrm{h}}(i+1,\, j)\big) - \delta^r V_r^{\mathrm{h}}\big(\chi^{\mathrm{h}}(i,j)\big) \\
&\quad = \chi^{\mathrm{h}\mathrm{T}}(i+1,\, j) Q_r^{\mathrm{h}} \chi^{\mathrm{h}}(i+1,\, j) - \delta^r \chi^{\mathrm{h}\mathrm{T}}(i,j) Q_r^{\mathrm{h}} \chi^{\mathrm{h}}(i,j) \\
&\quad = \zeta^{\mathrm{T}}(i,j) \big[E_1^{\mathrm{T}} Q_r^{\mathrm{h}} E_1 - \delta^r E_3^{\mathrm{T}} Q_r^{\mathrm{h}} E_3\big] \zeta(i,j),
\end{aligned} \tag{12}$$

$$\begin{aligned}
&\Delta V_r^{\mathrm{v}}\big(\chi^{\mathrm{v}}(i,j)\big) - (\delta^r - 1)V_r^{\mathrm{v}}\big(\chi^{\mathrm{v}}(i,j)\big)\\
&\quad = V_r^{\mathrm{v}}\big(\chi^{\mathrm{v}}(i,\, j+1)\big) - \delta^r V_r^{\mathrm{v}}\big(\chi^{\mathrm{v}}(i,j)\big)\\
&\quad = \chi^{\mathrm{v}\mathrm{T}}(i,\, j+1)Q_r^{\mathrm{v}}\chi^{\mathrm{v}}(i,\, j+1) - \delta^r \chi^{\mathrm{v}\mathrm{T}}(i,j)Q_r^{\mathrm{v}}\chi^{\mathrm{v}}(i,j)\\
&\quad = \zeta^{\mathrm{T}}(i,j)\big[E_2^{\mathrm{T}}Q_r^{\mathrm{v}}E_2 - \delta^r E_4^{\mathrm{T}}Q_r^{\mathrm{v}}E_4\big]\zeta(i,j). \qquad (13)
\end{aligned}$$

From (9) we obtain

$$\begin{aligned}
&\zeta^{\mathrm{T}}(i,j)E_1^{\mathrm{T}}\big(\mathcal{A}^r E_3 + \mathcal{B}^r E_4 + \mathcal{E}^r E_5 - E_1\big)\zeta(i,j) = 0,\\
&\zeta^{\mathrm{T}}(i,j)E_2^{\mathrm{T}}\big(\mathcal{C}^r E_3 + \mathcal{D}^r E_4 + \mathcal{F}^r E_5 - E_2\big)\zeta(i,j) = 0.
\end{aligned} \qquad (14)$$

From (14) we get

$$\begin{aligned}
&\zeta^{\mathrm{T}}(i,j)\,\mathrm{sym}\big\{E_1^{\mathrm{T}}\mathcal{A}^r E_3 + E_1^{\mathrm{T}}\mathcal{B}^r E_4 + E_1^{\mathrm{T}}\mathcal{E}^r E_5 - E_1^{\mathrm{T}}E_1\big\}\zeta(i,j) \geqslant 0,\\
&\zeta^{\mathrm{T}}(i,j)\,\mathrm{sym}\big\{E_2^{\mathrm{T}}\mathcal{C}^r E_3 + E_2^{\mathrm{T}}\mathcal{D}^r E_4 + E_2^{\mathrm{T}}\mathcal{F}^r E_5 - E_2^{\mathrm{T}}E_2\big\}\zeta(i,j) \geqslant 0.
\end{aligned} \qquad (15)$$

By the ETC condition (4), we obtain

$$\begin{aligned}
&\xi^r\zeta^{\mathrm{T}}(i,j)\big\{\big[C_1^r E_6 + C_2^r E_7 + E_5\big]^{\mathrm{T}}\Theta^r\big[C_1^r E_6 + C_2^r E_7 + E_5\big]\\
&\quad - E_5^{\mathrm{T}}\Theta^r E_5\big\}\zeta(i,j) + \frac{1}{2}\gamma\delta^{\lambda t} \geqslant 0. \qquad (16)
\end{aligned}$$

From (12), (13), (15), and (16) we derive

$$\begin{aligned}
&V_r\big(\chi^*(i,j)\big) - \delta^r\big(V_r^{\mathrm{h}}\big(\chi^{\mathrm{h}}(i,j)\big) + V_r^{\mathrm{v}}\big(\chi^{\mathrm{v}}(i,j)\big)\big)\\
&\quad \leqslant \zeta^{\mathrm{T}}(i,j)\Xi^r\zeta(i,j) + \frac{1}{2}\gamma\delta^{\lambda t}, \qquad (17)
\end{aligned}$$

where

$$\begin{aligned}
\Xi^r = {}& E_1^{\mathrm{T}}Q_r^{\mathrm{h}}E_1 + E_2^{\mathrm{T}}Q_r^{\mathrm{v}}E_2 - \delta^r E_3^{\mathrm{T}}Q_r^{\mathrm{h}}E_3 - \delta^r E_4^{\mathrm{T}}Q_r^{\mathrm{v}}E_4 - \xi^r E_5^{\mathrm{T}}\Theta^r E_5\\
&+ \mathrm{sym}\big\{E_1^{\mathrm{T}}\mathcal{A}^r E_3 + E_1^{\mathrm{T}}\mathcal{B}^r E_4 + E_1^{\mathrm{T}}\mathcal{E}^r E_5 - E_1^{\mathrm{T}}E_1\big\}\\
&+ \mathrm{sym}\big\{E_2^{\mathrm{T}}\mathcal{C}^r E_3 + E_2^{\mathrm{T}}\mathcal{D}^r E_4 + E_2^{\mathrm{T}}\mathcal{F}^r E_5 - E_2^{\mathrm{T}}E_2\big\}\\
&+ \xi^r\big[C_1^r E_6 + C_2^r E_7 + E_5\big]^{\mathrm{T}}\Theta^r\big[C_1^r E_6 + C_2^r E_7 + E_5\big].
\end{aligned}$$

By applying the Schur complement lemma, $\Xi^r < 0$ corresponds to

$$\hat{\Upsilon}^r = \begin{pmatrix} \hat{\Upsilon}_{11}^r & \hat{\Upsilon}_{12}^r \\ * & \Pi^r \end{pmatrix} < 0, \qquad (18)$$

where

$$\begin{aligned}
\hat{\Upsilon}_{11}^r &= \mathrm{diag}\big(-\big(Q_r^{\mathrm{h}}\big)^{-1}, -\big(Q_r^{\mathrm{v}}\big)^{-1}, -\big(\xi^r\Theta^r\big)^{-1}\big),\\
\hat{\Upsilon}_{12}^r &= \big(E_1^{\mathrm{T}},\, E_2^{\mathrm{T}},\, \big(C_1^r E_6 + C_2^r E_7 + E_5\big)^{\mathrm{T}}\big)^{\mathrm{T}},\\
\Pi^r &= \mathrm{sym}\big\{E_1^{\mathrm{T}}\mathcal{A}^r E_3 + E_1^{\mathrm{T}}\mathcal{B}^r E_4 + E_1^{\mathrm{T}}\mathcal{E}^r E_5 - E_1^{\mathrm{T}}E_1\big\}\\
&\quad + \mathrm{sym}\big\{E_2^{\mathrm{T}}\mathcal{C}^r E_3 + E_2^{\mathrm{T}}\mathcal{D}^r E_4 + E_2^{\mathrm{T}}\mathcal{F}^r E_5 - E_2^{\mathrm{T}}E_2\big\}\\
&\quad - \delta^r E_3^{\mathrm{T}}Q_r^{\mathrm{h}}E_3 - \delta^r E_4^{\mathrm{T}}Q_r^{\mathrm{v}}E_4 - \xi^r E_5^{\mathrm{T}}\Theta^r E_5.
\end{aligned}$$

Multiplying (18) from the left by $\operatorname{diag}(U_1^r, U_2^r, W^r, I_c)$ and from the right by $\operatorname{diag}(U_1^{r\mathrm{T}}, U_2^{r\mathrm{T}}, W^{r\mathrm{T}}, I_c)$ with $c = 2(n_{\mathrm{h}} + n_{\hat{h}} + n_{\mathrm{v}} + n_{\hat{v}}) + n_l$, then we get

$$\check{\Upsilon}_r = \begin{pmatrix} \check{\Upsilon}_{11r} & \check{\Upsilon}_{12r} \\ * & \mathit{\Pi}^r \end{pmatrix} < 0, \tag{19}$$

where

$$\begin{aligned} \check{\Upsilon}_{11r} &= \operatorname{diag}\big(-U_1^r (Q_r^{\mathrm{h}})^{-1} U_1^{r\mathrm{T}},\ -U_2^r (Q_r^{\mathrm{v}})^{-1} U_2^{r\mathrm{T}},\ -W^r (\xi^r \Theta^r)^{-1} W^{r\mathrm{T}}\big), \\ \check{\Upsilon}_{12r} &= \big(\big(U_1^r E_1\big)^{\mathrm{T}},\ \big(U_2^r E_2\big)^{\mathrm{T}},\ \big(W^r \big(C_1^r E_6 + C_2^r E_7 + E_5\big)\big)^{\mathrm{T}}\big)^{\mathrm{T}}. \end{aligned}$$

Using the inequalities

$$\begin{aligned} -U_1^r \big(Q_r^{\mathrm{h}}\big)^{-1} U_1^{r\mathrm{T}} &\leqslant Q_r^{\mathrm{h}} - U_1^r - U_1^{r\mathrm{T}}, \\ -U_2^r \big(Q_r^{\mathrm{v}}\big)^{-1} U_2^{r\mathrm{T}} &\leqslant Q_r^{\mathrm{v}} - U_2^r - U_2^{r\mathrm{T}}, \\ -W^r \big(\xi^r \Theta^r\big)^{-1} W^{r\mathrm{T}} &\leqslant \xi^r \Theta^r - W^r - W^{r\mathrm{T}}, \end{aligned}$$

we obtain

$$\begin{aligned} \Upsilon^r = &\begin{pmatrix} Q_r^{\mathrm{h}} - U_1^r - U_1^{r\mathrm{T}} & 0 & 0 & U_1^r E_1 \\ * & Q_r^{\mathrm{v}} - U_2^r - U_2^{r\mathrm{T}} & 0 & U_2^r E_2 \\ * & * & \xi^r \Theta^r - W^r - W^{r\mathrm{T}} & W^r (C_1^r E_6 + C_2^r E_7 + E_5) \\ * & * & * & \mathit{\Pi}^r \end{pmatrix} \\ &< 0. \end{aligned}$$

When $\Upsilon^r < 0$, the condition given by (19) is satisfied, implying that $\Xi^r < 0$. Based on (17), it can be observed that when $t = i + j$ falls within the interval $[t_{s-1}, t_s)$, we may conclude that

$$V_r\big(\chi^*(i,j)\big) \leqslant \delta^r V_r\big(\chi(i,j)\big) + \frac{1}{2}\gamma \delta^{\lambda t}.$$

Consider the scenario where a positive scalar $\breve{\delta}^r$, which is sufficiently small, exists for any $r \in M$ such that

$$\sum_{r=1}^{N} \bar{\epsilon}^r \left[\frac{\ln \beta^r}{\gamma^r} + \ln \tilde{\delta}^r\right] < 0, \tag{20}$$

$$V_r\big(\chi^*(i,j)\big) \leqslant \big(\tilde{\delta}^r - \breve{\delta}^r\big) V_r\big(\chi(i,j)\big) + \frac{1}{2}\gamma \delta^{\lambda t}, \tag{21}$$

where $\tilde{\delta}^r = \delta^r + \breve{\delta}^r$. Let

$$\eta(t) = \max\left\{\eta_r(t) = \sqrt{\frac{\frac{1}{2}\gamma \delta^{\lambda t}}{\breve{\delta}^r [\lambda_{\max}(Q_r^{\mathrm{h}}) + \lambda_{\max}(Q_r^{\mathrm{v}})]}},\ r \in M\right\}.$$

Given that $\|\chi(i,j)\| \geqslant \eta(t)$ for $t = i + j$, it follows from (21) that

$$V_r\big(\chi^*(i,j)\big) \leqslant \tilde{\delta}^r V_r\big(\chi(i,j)\big). \tag{22}$$

Therefore, from (22) we have

$$\begin{aligned} V_r\big(\chi^*(1,t)\big) &\leqslant \tilde{\delta}^r\big[V_r^{\mathrm{h}}\big(\chi(0,t)\big) + V_r^{\mathrm{v}}\big(\chi(1,\,t-1)\big)\big],\\ V_r\big(\chi^*(2,t-1)\big) &\leqslant \tilde{\delta}^r\big[V_r^{\mathrm{h}}\big(\chi(1,\,t-1)\big) + V_r^{\mathrm{v}}\big(\chi(2,\,t-2)\big)\big],\\ &\cdots,\\ V_r\big(\chi^*(t,1)\big) &\leqslant \tilde{\delta}^r\big[V_r^{\mathrm{h}}\big(\chi(t-1,\,1)\big) + V_r^{\mathrm{v}}\big(\chi(t,0)\big)\big]. \end{aligned} \tag{23}$$

From (22) and (23) we obtain the following:

$$\sum_{t+1=i+j} V_r(\chi^*(i,j)) \leqslant \tilde{\delta}^r \sum_{t=i+j} V_r\big(\chi(i,j)\big). \tag{24}$$

By (11) and (24), when $t = i + j \in [t_{s-1}, t_s)$, we have

$$\begin{aligned} \sum_{t=i+j} V_{\alpha(t)}\big(\chi(i,j)\big) &< \tilde{\delta}^{\alpha(t-1)} \sum_{t-1=i+j} V_{\alpha(t-1)}\big(\chi(i,j)\big)\\ &< \tilde{\delta}_{t-t_{\kappa-1}}^{\alpha(t_{\kappa-1})} \sum_{t_{\kappa-1}=i+j} V_{\alpha(t_{\kappa-1})}\big(\chi(i,j)\big)\\ &< \beta^{\alpha(t_{\kappa-1})}\tilde{\delta}_{t-t_{\kappa-1}}^{\alpha(t_\kappa-1)} \sum_{t_{\kappa-1}=i+j} V_{\alpha(t_{\kappa-1})}\big(\chi(i,j)\big)\\ &< \beta^{\alpha(t_{\kappa-1})}\tilde{\delta}_{t-t_{\kappa-1}}^{\alpha(t_{\kappa-1})}\tilde{\delta}_{t_{\kappa-1}-t_{s-2}}^{\alpha(t_{s-2})} \sum_{t_{s-2}=i+j} V_{\alpha(t_{s-2})}\big(\chi(i,j)\big)\\ &< \cdots < \prod_{r=1}^{N} \beta_{N^r(t)}^r \tilde{\delta}_{T^r(t)}^r \sum_{0=i+j} V_{\alpha(0)}\big(\chi(i,j)\big). \end{aligned}$$

Thus,

$$\widetilde{\lambda} \sum_{t=i+j} \big\|\chi(i,j)\big\| < \prod_{r=1}^{N} \beta_{N^r(t)}^r \tilde{\delta}_{T^r(t)}^r \sum_{0=i+j} V_{\alpha(0)}\big(\chi(i,j)\big),$$

where $\widetilde{\lambda} = \min\{\lambda_{\max}(Q_r^{\mathrm{h}}) + \lambda_{\max}(Q_r^{\mathrm{v}}),\ r \in M\}$, and $N^r(t)$ represents the number of times the system switches to mode $r$ within the time interval $[t_{s-1}, t_s)$. Therefore, we have

$$\begin{aligned} \frac{\ln\eta(t) - \ln\widetilde{\lambda}}{t} \leqslant \frac{\ln\sum_{t=i+j}\|\chi(i,j)\|}{t} < \frac{\ln\sum_{0=i+j} V_{\alpha(0)}(\chi(i,j)) - \ln\widetilde{\lambda}}{t}\\ + \sum_{r=1}^{N}\left[\frac{N^r(t)}{t}\ln\beta^r + \frac{T^r(t)}{t}\ln\tilde{\delta}^r\right]. \end{aligned} \tag{25}$$

According to (20),

$$\lim_{t\to\infty}\frac{N^r(t)}{t} = \lim_{t\to\infty}\frac{\frac{T^r(t)}{t}}{\frac{T^r(t)}{N^r(t)}} = \frac{\bar{\epsilon}^r}{\gamma^r}. \tag{26}$$

In (25), because

$$\begin{aligned}&\limsup_{t\to\infty}\left\{\frac{\ln\sum_{0=i+j}V_{\alpha(0)}(\chi(i,j))-\ln\widetilde{\lambda}}{t}+\sum_{r=1}^{N}\left[\frac{N^r(t)}{t}\ln\beta^r+\frac{T^r(t)}{t}\ln\tilde{\delta}^r\right]\right\}\\&=\limsup_{t\to\infty}\left\{\sum_{r=1}^{N}\left[\frac{N^r(t)}{t}\ln\beta^r+\frac{T^r(t)}{t}\ln\tilde{\delta}^r\right]\right\}=\sum_{r=1}^{R}\left[\frac{\bar{\epsilon}^r}{\gamma^r}\left[\ln\beta^r+\ln\tilde{\delta}^r\right]\right]\\&<0,\end{aligned}\tag{27}$$

so,

$$\limsup_{t\to\infty}\frac{\ln\eta(t)-\ln\widetilde{\lambda}}{t}<0.\tag{28}$$

From (25)–(28) we can derive that

$$\limsup_{t\to\infty}\frac{\ln\sum_{t=i+j}\|\chi(i,j)\|}{t}<0,$$

indicating that the error system (3) achieves the GES. □

**Remark 4.** Unlike the mode-independent event-triggered strategy in [22] for 2-D switched systems, our method removes the constraint of fixed sampling intervals on mode dwell time, as each mode's initial sampling instant aligns with its switching time. This enables flexible adjustment of sampling intervals, free from traditional fixed-interval rules.

**Remark 5.** Theorem 1 applies to switched systems with ADT and minimal dwell time. Unlike [22], which requires ADT to exceed a preset threshold for stability, our theory depends less on specific system parameters, thus offering broader applicability, higher practicality, and enhanced flexibility in synchronizing and controlling 2-D discrete-time switched systems.

Based on Theorem 1, we will outline the specific control gain parameters necessary for the synchronization controller designed for the error system (3). We let

$$\widetilde{\mathcal{A}}^r=\begin{pmatrix}A_{11}^r & 0_{n_{\mathrm{h}}\times n_{\hat{h}}}\\ 0_{n_{\hat{h}}\times n_{\mathrm{h}}} & 0_{n_{\hat{h}}\times n_{\hat{h}}}\end{pmatrix},\qquad \widetilde{\mathcal{B}}^r=\begin{pmatrix}A_{12}^r & 0_{n_{\mathrm{h}}\times n_{\hat{v}}}\\ 0_{n_{\hat{h}}\times n_{\mathrm{v}}} & 0_{n_{\hat{h}}\times n_{\hat{v}}}\end{pmatrix},$$

$$\widetilde{\mathcal{C}}^r=\begin{pmatrix}A_{21}^r & 0_{n_{\mathrm{v}}\times n_{\hat{h}}}\\ 0_{n_{\hat{v}}\times n_{\mathrm{h}}} & 0_{n_{\hat{v}}\times n_{\hat{h}}}\end{pmatrix},\qquad \widetilde{\mathcal{D}}^r=\begin{pmatrix}A_{22}^r & 0_{n_{\mathrm{v}}\times n_{\hat{v}}}\\ 0_{n_{\hat{v}}\times n_{\mathrm{v}}} & 0_{n_{\hat{v}}\times n_{\hat{v}}}\end{pmatrix},$$

$$\mathcal{K}_1^r=\begin{pmatrix}\hat{A}_{11}^r & \hat{B}_1^r\\ \hat{C}_1^r & 0_{m\times n_l}\end{pmatrix},\qquad \mathcal{K}_2^r=\begin{pmatrix}\hat{A}_{12}^r & \hat{B}_1^r\\ \hat{C}_2^r & 0_{m\times n_l}\end{pmatrix},$$

$$\mathcal{K}_3^r=\begin{pmatrix}\hat{A}_{21}^r & \hat{B}_2^r\\ \hat{C}_1^r & 0_{m\times n_l}\end{pmatrix},\qquad \mathcal{K}_4^r=\begin{pmatrix}\hat{A}_{22}^r & \hat{B}_2^r\\ \hat{C}_2^r & 0_{m\times n_l}\end{pmatrix},$$

$$\mathcal{P}_1^r=\begin{pmatrix}0_{n_{\mathrm{h}}\times n_{\hat{h}}} & B_1^r[I_m+\varpi^r]\\ I_{n_{\hat{h}}} & 0_{n_{\hat{h}}\times m}\end{pmatrix},\qquad \mathcal{P}_2^r=\begin{pmatrix}0_{n_{\mathrm{v}}\times n_{\hat{v}}} & B_2^r[I_m+\varpi^r]\\ I_{n_{\hat{v}}} & 0_{n_{\hat{v}}\times m}\end{pmatrix},$$

$$\mathcal{Q}_1^r = \begin{pmatrix} 0_{n_{\hat{h}} \times n_{\mathrm{h}}} & I_{n_{\hat{h}}} \\ C_1^r & 0_{n_l \times n_{\hat{h}}} \end{pmatrix}, \qquad \mathcal{Q}_2^r = \begin{pmatrix} 0_{n_{\hat{v}} \times n_{\mathrm{v}}} & I_{n_{\hat{v}}} \\ C_2^r & 0_{n_l \times n_{\hat{v}}} \end{pmatrix},$$
$$\mathcal{E}_1^r = \begin{pmatrix} 0_{n_{\mathrm{h}} \times n_{\hat{h}}} & 0_{n_{\mathrm{h}} \times m} \\ I_{n_{\hat{h}}} & 0_{n_{\hat{h}} \times m} \end{pmatrix}, \qquad \mathcal{E}_2^r = \begin{pmatrix} 0_{n_{\hat{h}} \times n_l} \\ I_{n_l} \end{pmatrix},$$
$$\mathcal{F}_1^r = \begin{pmatrix} 0_{n_{\mathrm{v}} \times n_{\hat{v}}} & 0_{n_{\mathrm{v}} \times m} \\ I_{n_{\hat{v}}} & 0_{n_{\hat{v}} \times m} \end{pmatrix}, \qquad \mathcal{F}_2^r = \begin{pmatrix} 0_{n_{\hat{h}} \times n_l} \\ I_{n_l} \end{pmatrix}.$$

Then we can obtain

$$\mathcal{A}^r = \widetilde{\mathcal{A}}^r + \mathcal{P}_1^r \mathcal{K}_1^r \mathcal{Q}_1^r, \qquad \mathcal{B}^r = \widetilde{\mathcal{B}}^r + \mathcal{P}_1^r \mathcal{K}_2^r \mathcal{Q}_2^r, \qquad \mathcal{C}^r = \widetilde{\mathcal{C}}^r + \mathcal{P}_2^r \mathcal{K}_3^r \mathcal{Q}_1^r,$$
$$\mathcal{D}^r = \widetilde{\mathcal{D}}^r + \mathcal{P}_2^r \mathcal{K}_4^r \mathcal{Q}_2^r, \qquad \mathcal{E}^r = \mathcal{E}_1^r \mathcal{K}_1^r \mathcal{E}_2^r, \qquad \mathcal{F}^r = \mathcal{F}_1^r \mathcal{K}_3^r \mathcal{F}_2^r.$$

Therefore, $\Upsilon^r < 0$ is equivalent to $\Phi^r < 0$, i.e.,

$$\Phi^r = \begin{pmatrix} \Phi_{11}^r & \Phi_{12}^r \\ * & \Phi_{22}^r \end{pmatrix} < 0,$$

where

$$\begin{aligned}
\Phi_{11}^r &= \operatorname{diag}\big(Q_r^{\mathrm{h}} - U_1^r - U_1^{r\mathrm{T}},\, Q_r^{\mathrm{v}} - U_2^r - U_2^{r\mathrm{T}},\, \xi^r \Theta^r - W^r - W^{r\mathrm{T}}\big), \\
\Phi_{12}^r &= \big(\big(U_1^r E_1\big)^{\mathrm{T}},\, \big(U_2^r E_2\big)^{\mathrm{T}},\, \big(W^r \big(C_1^r E_6 + C_2^r E_7 + E_5\big)\big)^{\mathrm{T}}\big)^{\mathrm{T}}, \\
\Phi_{22}^r &= \operatorname{sym}\big\{E_1^{\mathrm{T}} \mathcal{A}_1^r E_3 + E_1^{\mathrm{T}} \mathcal{B}_1^r E_4 + E_2^{\mathrm{T}} \mathcal{C}_1^r E_3 + E_2^{\mathrm{T}} \mathcal{D}_1^r E_4 - E_1^{\mathrm{T}} E_1 - E_2^{\mathrm{T}} E_2\big\} \\
&\quad + \operatorname{sym}\big\{E_1^{\mathrm{T}} \mathcal{P}_1^r \mathcal{K}_1^r \mathcal{Q}_1^r E_3 + E_1^{\mathrm{T}} \mathcal{P}_1^r \mathcal{K}_2^r \mathcal{Q}_2^r E_4 + E_1^{\mathrm{T}} \mathcal{E}_1^r \mathcal{K}_1^r \mathcal{E}_2^r E_5\big\} \\
&\quad + \operatorname{sym}\big\{E_2^{\mathrm{T}} \mathcal{P}_2^r \mathcal{K}_3^r \mathcal{Q}_1^r E_3 + E_2^{\mathrm{T}} \mathcal{P}_2^r \mathcal{K}_4^r \mathcal{Q}_2^r E_4 + E_2^{\mathrm{T}} \mathcal{F}_1^r \mathcal{K}_3^r \mathcal{F}_2^r E_5\big\} \\
&\quad - \delta^r E_3^{\mathrm{T}} Q_r^{\mathrm{h}} E_3 - \delta^r E_4^{\mathrm{T}} Q_r^{\mathrm{v}} E_4 - \xi^r E_5^{\mathrm{T}} \Theta^r E_5.
\end{aligned}$$

The quantization-based event-triggered dynamic output controller for the error system (3) will be designed based on the following theorem.

**Theorem 2.** *Assume that the control gain matrices $\hat{A}_{11}^r$, $\hat{A}_{12}^r$, $\hat{A}_{21}^r$, $\hat{A}_{22}^r$, $\hat{B}_1^r$, $\hat{B}_2^r$, $\hat{C}_1^r$, $\hat{C}_2^r$ are all computable and Assumptions* 1 *and* 2 *are fulfilled. If for the predefined scalars $\delta^r > 0$, $\beta^r \geqslant 1$, there exist matrices $0 < Q_r^{\mathrm{h}} \in \mathbb{R}^{(n_{\mathrm{h}}+n_{\hat{h}}) \times (n_{\mathrm{h}}+n_{\hat{h}})}$, $0 < Q_r^{\mathrm{v}} \in \mathbb{R}^{(n_{\mathrm{v}}+n_{\hat{v}}) \times (n_{\mathrm{v}}+n_{\hat{v}})}$, $0 < \Theta^r \in \mathbb{R}^{n_l \times n_l}$ and invertible matrices $U_1^r \in \mathbb{R}^{(n_{\mathrm{h}}+n_{\hat{h}}) \times (n_{\mathrm{h}}+n_{\hat{h}})}$, $U_2^r \in \mathbb{R}^{(n_{\mathrm{v}}+n_{\hat{v}}) \times (n_{\mathrm{v}}+n_{\hat{v}})}$, $W^r \in \mathbb{R}^{n_l \times n_l}$ such that*

$$\Phi^r < 0, \tag{29}$$
$$Q_r^{\mathrm{h}} - U_1^r - U_1^{r\mathrm{T}} < 0, \qquad Q_r^{\mathrm{v}} - U_2^r - U_2^{r\mathrm{T}} < 0, \qquad \xi^r \Theta^r - W^r - W^{r\mathrm{T}} < 0,$$

*then upon application of the controller specified in* (5)*, the error system described by* (3) *achieves the GES. Furthermore, the control gain matrices within controller* (5) *and the event-triggered parameters $\Theta^r$ defined in the event-triggered condition* (4) *can be obtained through solving LMI given in* (29)*.*

*Proof.* Since (10) is equivalent to (29), the proof is similar to that of Theorem 1. □

## 4 Numerical example: Synchronization of a master-slave robotic arm collaborative assembly system

Within this part, we introduce a detailed numerical simulation example of 2-D discrete-time switched master-slave Roesser systems with three modes ($M = 3$). The purpose of these examples is to showcase the performance and reliability of the proposed event-triggered controller when applied to system (3).

A master-slave manipulator system for engine block assembly aims to ensure precise trajectory and intention consistency between master and slave arms. It operates in 3 modes: positioning (Mode 1), pre-tightening (Mode 2), and tightening (Mode 3). A 2-D discrete-time switched system based on the Roesser model is established with the error dynamic equation given by (3), and system coefficient matrices are provided as follows:

Mode 1:

$$A^1 = \begin{bmatrix} A_{11}^1 & A_{12}^1 \\ A_{21}^1 & A_{22}^1 \end{bmatrix} = \begin{bmatrix} 0.88 & 0.3 \\ 0.2 & -1.2 \end{bmatrix},$$

$$B^1 = \begin{bmatrix} B_1^1 \\ B_2^1 \end{bmatrix} = \begin{bmatrix} 0.5 \\ 0.2 \end{bmatrix}, \qquad C^1 = \begin{bmatrix} C_1^1 \\ C_2^1 \end{bmatrix}^{\mathrm{T}} = \begin{bmatrix} 0.5 \\ 0.2 \end{bmatrix}^{\mathrm{T}}.$$

Mode 2:

$$A^2 = \begin{bmatrix} A_{11}^2 & A_{12}^2 \\ A_{21}^2 & A_{22}^2 \end{bmatrix} = \begin{bmatrix} 0.8 & 0.5 \\ 0.3 & 0.4 \end{bmatrix},$$

$$B^2 = \begin{bmatrix} B_1^2 \\ B_2^2 \end{bmatrix} = \begin{bmatrix} 0.3 \\ 0.2 \end{bmatrix}, \qquad C^2 = \begin{bmatrix} C_1^2 \\ C_2^2 \end{bmatrix}^{\mathrm{T}} = \begin{bmatrix} 0.2 \\ 0.2 \end{bmatrix}^{\mathrm{T}}.$$

Mode 3:

$$A^3 = \begin{bmatrix} A_{11}^3 & A_{12}^3 \\ A_{21}^3 & A_{22}^3 \end{bmatrix} = \begin{bmatrix} 0.95 & 0.56 \\ 0.5 & 1.1 \end{bmatrix},$$

$$B^3 = \begin{bmatrix} B_1^3 \\ B_2^3 \end{bmatrix} = \begin{bmatrix} 0.4 \\ 0.3 \end{bmatrix}, \qquad C^3 = \begin{bmatrix} C_1^3 \\ C_2^3 \end{bmatrix}^{\mathrm{T}} = \begin{bmatrix} 0.2 \\ 0.1 \end{bmatrix}^{\mathrm{T}}.$$

Let the initial conditions for systems (1), (2), and (3) be set as follows:

$$x^{\mathrm{h}}(0,j) = x^{\mathrm{h}}(j,0) = \begin{cases} \operatorname{rand} 2 + 0.8 \sin j & \text{if } 0 \leqslant j \leqslant 21, \\ 0 & \text{if } j > 21, \end{cases}$$

$$x^{\mathrm{v}}(0,j) = x^{\mathrm{v}}(j,0) = \begin{cases} \operatorname{rand} 2 + 0.9 \cos j & \text{if } 0 \leqslant j \leqslant 21, \\ 0 & \text{if } j > 21, \end{cases}$$

$$\widetilde{x}^{\mathrm{h}}(0,j) = \widetilde{x}^{\mathrm{h}}(j,0) = \begin{cases} \operatorname{rand} 4 + 1.2 \sin j & \text{if } 0 \leqslant j \leqslant 21, \\ 0 & \text{if } j > 21, \end{cases}$$

$$\widetilde{x}^{\mathrm{v}}(0,j) = \widetilde{x}^{\mathrm{v}}(j,0) = \begin{cases} \operatorname{rand} 6 + 1.4 \cos j & \text{if } 0 \leqslant j \leqslant 21, \\ 0 & \text{if } j > 21, \end{cases}$$

$$e^{\mathrm{h}}(0,j)=\widetilde{x}^{\mathrm{h}}(0,j)-x^{\mathrm{h}}(0,j), \qquad e^{\mathrm{h}}(j,0)=\widetilde{x}^{\mathrm{h}}(j,0)-x^{\mathrm{h}}(j,0),$$
$$e^{\mathrm{v}}(0,j)=\widetilde{x}^{\mathrm{v}}(0,j)-x^{\mathrm{v}}(0,j), \qquad e^{\mathrm{v}}(j,0)=\widetilde{x}^{\mathrm{v}}(j,0)-x^{\mathrm{v}}(j,0).$$

Under Assumption 1, the switching signal is specified as $\alpha(i,j)=\alpha(t)$, $i,j\in\mathbb{N}$. The TPM is given by

$$\mathcal{J}=\begin{bmatrix}0 & 0.4 & 0.6\\ 0.5 & 0 & 0.5\\ 0.3 & 0.7 & 0\end{bmatrix}.$$

Given that the unique stationary distribution of $\mathcal{J}$ is determined to be $\epsilon=(0.2863, 0.3612, 0.3524)$, and by setting $\xi^1=0.7$, $\xi^2=0.8$, $\xi^3=0.9$, $\gamma=1.2$, $\delta=0.4$, and $\lambda=4$, a feasible solution to the LMIs, in accordance with Theorem 2, is derived. This yields the control gain matrices for the controller (5), including the positive definite matrices $Q_r^{\mathrm{h}}$ and $Q_r^{\mathrm{v}}$ as follows:

Mode 1:

$$\hat{A}_{11}^1=0.0058, \quad \hat{A}_{12}^1=-0.0012, \quad \hat{A}_{21}^1=0.0129, \quad \hat{A}_{22}^1=-0.0029,$$
$$\hat{B}_1^1=0.0006, \quad \hat{B}_2^1=0.0031, \quad \hat{C}_1^1=-0.0028, \quad \hat{C}_2^1=-0.0002,$$
$$Q_1^{\mathrm{h}}=\begin{pmatrix}0.7806 & 0.0003\\ 0.0003 & 0.7260\end{pmatrix}, \qquad Q_1^{\mathrm{v}}=\begin{pmatrix}0.8151 & -0.0000\\ -0.0000 & 0.7254\end{pmatrix}.$$

Mode 2:

$$\hat{A}_{11}^2=0.0007, \quad \hat{A}_{12}^2=-0.0003, \quad \hat{A}_{21}^2=-0.0041, \quad \hat{A}_{22}^2=0.0011,$$
$$\hat{B}_1^2=0.0003, \quad \hat{B}_2^2=-0.0010, \quad \hat{C}_1^2=0.0040, \quad \hat{C}_2^2=0.0015,$$
$$Q_2^{\mathrm{h}}=\begin{pmatrix}0.8059 & 0.0003\\ 0.0003 & 0.7538\end{pmatrix}, \qquad Q_2^{\mathrm{v}}=\begin{pmatrix}0.8321 & 0.0001\\ 0.0001 & 0.7532\end{pmatrix}.$$

Mode 3:

$$\hat{A}_{11}^3=-0.0007\cdot10^{-3}, \quad \hat{A}_{12}^3=-0.0051, \quad \hat{A}_{21}^3=-0.0025, \quad \hat{A}_{22}^3=0.0065,$$
$$\hat{B}_1^3=-0.2301\cdot10^{-3}, \quad \hat{B}_2^3=0.0006, \quad \hat{C}_1^3=0.7628\cdot10^{-3}, \quad \hat{C}_2^3=0.0001,$$
$$Q_3^{\mathrm{h}}=\begin{pmatrix}0.8269 & 0.0004\\ 0.0004 & 0.7742\end{pmatrix}, \qquad Q_3^{\mathrm{v}}=\begin{pmatrix}0.8564 & 0.0001\\ 0.0001 & 0.7738\end{pmatrix}.$$

Given the computed trigger parameters for the ETC condition (4) as $\Theta_1=0.1532$, $\Theta_2=0.0926$, and $\Theta_3=0.0667$.

Figures 1 and 2 depict the state trajectories of the master and slave systems, respectively, under the switching signal illustrated in Fig. 3. Figure 4 specifically characterizes the synchronization error dynamics between the master and slave systems, illustrating their evolution over the two dimensions of the Roesser model.

To validate the efficacy of the designed controller in achieving synchronization, the identical switching signal from Fig. 3 was applied, ensuring consistent experimental conditions. The state responses of the controlled error system (Fig. 5) demonstrate that

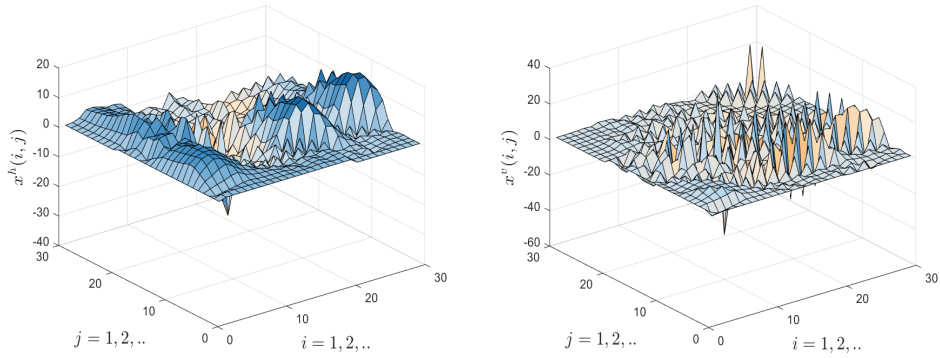


(a) State response $x^{\mathrm{h}}(i,j)$ (b) State response $x^{\mathrm{v}}(i,j)$

**Figure 1.** Evolution of state response in 2-D switched master system.

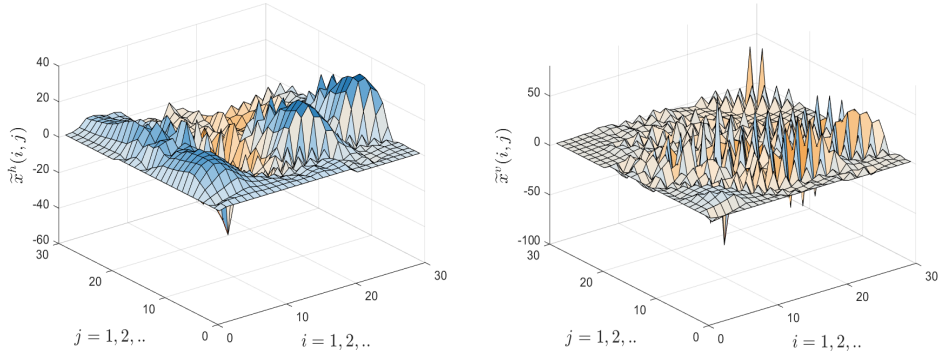


(a) State response $\widetilde{x}^{\mathrm{h}}(i,j)$ without control (b) State response $\widetilde{x}^{\mathrm{v}}(i,j)$ without control

**Figure 2.** Evolution of state response in 2-D switched slave system without control.

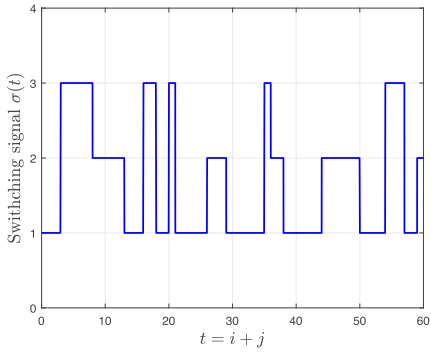


**Figure 3.** Switching signal.

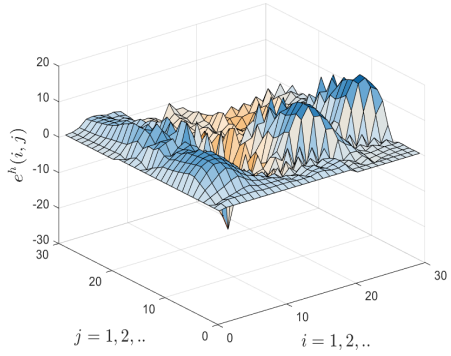


(a) State response $e^{\mathrm{h}}(i,j)$ without control

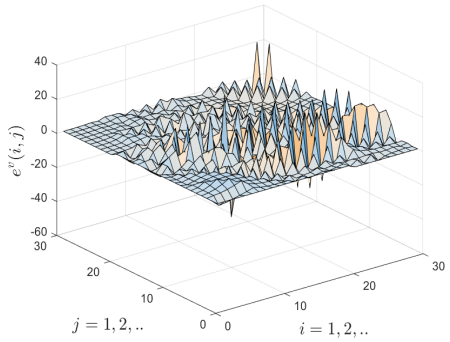


(b) State response $e^{\mathrm{v}}(i,j)$ without control

**Figure 4.** Evolution of state response in 2-D switched error system without control.

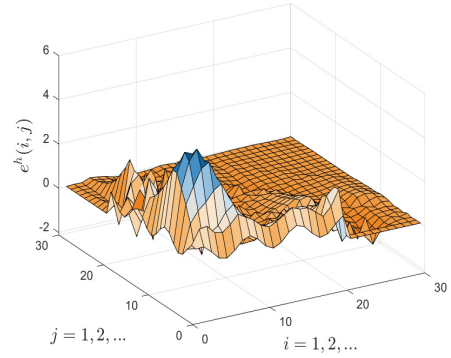


(a) State response $e^{\mathrm{h}}(i,j)$ under the action of controller

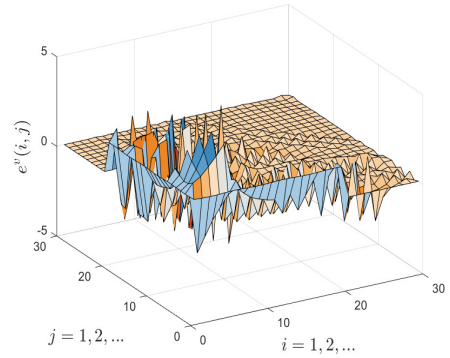


(b) State response $e^{\mathrm{v}}(i,j)$ under the action of controller

**Figure 5.** Evolution of state response in 2-D switched error system with controller.

the designed controller effectively stabilizes system (3). Comparative analysis of Figs. 4 and 5 demonstrates that the proposed controller can swiftly achieve master-slave synchronization.

Further evidence of the controller's performance is provided in Fig. 6, which plots the event-triggered transmission times and intervals. This figure highlights a significant advantage of the proposed event-triggered control strategy: a marked reduction in network bandwidth utilization. Conventional time-triggered mechanisms typically necessitate higher transmission frequencies, resulting in greater bandwidth consumption. In contrast, the proposed event-triggered approach minimizes transmission instances, while maintaining synchronization performance, thereby optimizing communication efficiency and conserving network resources. The initial event-triggering instant corresponds to the coordinate $(0, 0)$.

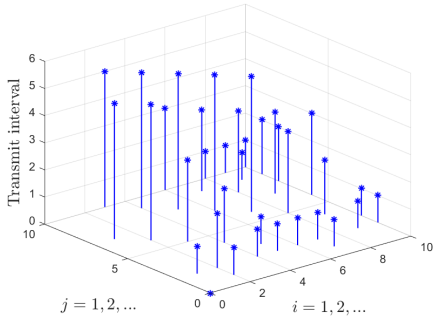


**Figure 6.** Event-triggered transmit intervals and transmit instants.

## 5 Conclusions

This study addresses synchronization control challenges in 2-D discrete-time switched master-slave systems in Roesser model under event-triggered strategies. It develops a mode-dependent event-triggered synchronization controller via quantization techniques to achieve GES. Given the unique complexity of 2-D discrete-time systems – especially with mode switching – existing research on synchronization and stabilization is limited, and the application of ETC in such systems remains nascent, making the design of innovative integrated control strategies particularly challenging.

A key advancement lies in formulating sufficient conditions for ensuring GES of 2-D discrete-time switched systems. Unlike prior methods requiring all modes to be stable, the proposed approach relaxes stability constraints, maintaining global stability even with unstable modes. These relaxed criteria expand the feasible region for LMI solutions and enhance computational tractability.

In numerical assessments, synchronization constraints in Theorem 2 (e.g., $\delta^r > 0$ and $\beta^r \geqslant 1$ for $r \in M$) are more generalized than strict conditions in previous studies ($\beta > 1$ with $\beta = \max\{\beta^r\}$ and $0 < \delta < 1$ with $\delta = \max\{\delta^r\}$), improving practical flexibility. Formulas like (29) in Theorem 2 enable direct computation of control gain matrices using MATLAB's LMI toolbox. Though ETC based on quantization is emerging, its network bandwidth-saving advantages have been validated, highlighting potential for efficient system resource utilization.

This work enriches the control theory of 2-D discrete-time switched systems, provides references for future research, and demonstrates the broad prospects of event-triggered dynamic output quantization control in designing efficient, stable systems.

**Conflicts of interest.** The authors declare no conflicts of interest.

## References

1. R.C. Budzinski, B.R.R. Boaretto, T.L. Prado, S.R. Lopes, Synchronization domains in two coupled neural networks, *Commun. Nonlinear Sci. Numer. Simul.*, **75**:140–151, 2019, `https://doi.org/10.1016/j.cnsns.2019.03.028`.

2. C. Chen, K. Xie, F.L. Lewis, S. Xie, R. Fierro, Adaptive synchronization of multi-agent systems with resilience to communication link faults, *Automatica*, **111**:108636, 2020, https://doi.org/10.1016/j.automatica.2019.108636.

3. Y. Dong, W. Lu, J. Chen, J. Cao, S. Xu, Adaptive neural network-based practical fixed-time consensus tracking for second-order nonlinear multi-agent systems with switching topologies, *Int. J. Robust Nonlinear Control*, **34**(12):8442–8464, 2024, https://doi.org/10.1002/rnc.7395.

4. H. Feng, Q. Song, S. Ma, W. Ma, C. Yin, D. Cao, H. Yu, A new adaptive sliding mode controller based on the RBF neural network for an electro-hydraulic servo system, *ISA Trans.*, **129**:472–484, 2022, https://doi.org/10.1016/j.isatra.2021.12.044.

5. X. Gao, E. Cui, D. Yang, Z. Tan, J. Sun, Adaptive displacement constraint control with predefined performance for active magnetic bearings, *IEEE Trans. Autom. Sci. Eng.*, **22**:883–894, 2025, https://doi.org/10.1109/TASE.2024.3355271.

6. Z. Han, W..K.S. Tang, Q. Jia, Event-triggered synchronization for nonlinear multi-agent systems with sampled data, *IEEE Trans. Circuits Syst. I Regul. Pap.*, **67**(10):3553–3561, 2020, https://doi.org/10.1109/TCSI.2020.2995194.

7. W. Huang, B. Tian, Y. Chen, J. Wang, Reachable set estimation of multi-agent systems with semi-Markov switching topologies and time-delay, *J. Franklin Inst.*, **360**(11):7415–7437, 2023, https://doi.org/10.1016/j.jfranklin.2023.05.022.

8. H. Li, Q. Wei, Data-driven optimal output cluster synchronization control of heterogeneous multi-agent systems, *IEEE Trans. Autom. Sci. Eng.*, **21**(3):3910–3920, 2024, https://doi.org/10.1109/TASE.2023.3289950.

9. L. Li, Y. Sun, J. Lu, J. Cao, Dynamic quantization driven synchronization of networked systems under event-triggered mechanism, *IEEE Trans. Circuits Syst. I Regul. Pap.*, **69**(4):1728–1740, 2021, https://doi.org/10.1109/TCSI.2021.3134989.

10. S. Li, C.K. Ahn, J. Guo, Z. Xiang, Neural network-based sampled-data control for switched uncertain nonlinear systems, *IEEE Trans. Syst. Man Cybern.: Syst.*, **51**(9):5437–5445, 2021, https://doi.org/10.1109/TSMC.2019.2954231.

11. J. Lian, C. Li, Event-triggered control for a class of switched uncertain nonlinear systems, *Syst. Control Lett.*, **135**:104592, 2020, https://doi.org/10.1016/j.sysconle.2019.104592.

12. J. Liang, Z. Wang, X. Liu, P. Louvieris, Robust synchronization for 2-D discrete-time coupled dynamical networks, *IEEE Trans. Neural Networks Learn. Syst.*, **23**(6):942–953, 2012, https://doi.org/10.1109/TNNLS.2012.2193414.

13. H. Lin, C. Wang, C. Chen, Y. Sun, C. Zhou, C. Xu, Q. Hong, Neural bursting and synchronization emulated by neural networks and circuits, *IEEE Trans. Circuits Syst. I Regul. Pap.*, **68**(8):3397–3410, 2021, https://doi.org/10.1109/TCSI.2021.3081150.

14. Y. Liu, Z. Fang, J.H. Park, F. Fang, Quantized event-triggered synchronization of discrete-time chaotic neural networks with stochastic deception attack, *IEEE Trans. Syst. Man Cybern.: Syst.*, **53**(7):4511–4521, 2023, https://doi.org/10.1109/TSMC.2023.3251355.

15. X. Qin, L. Shi, Y. Zou, Z. Tu, X. Xiong, X. Yang, Synchronization of discrete-time switched 2-D systems with Markovian topology via fault quantized output control, *Neural Process. Lett.*, **54**(1):165–180, 2022, https://doi.org/10.1007/s11063-021-10626-3.

16. C. Shang, W.-H. Chen, A.D. Stroock, F. You, Robust model predictive control of irrigation systems with active uncertainty learning and data analytics, *IEEE Trans. Control Syst. Technol.*, **28**(4):1493–1504, 2020, https://doi.org/10.1109/TCST.2019.2916753.

17. L. Tang, X.-Y. Zhang, Y.-J. Liu, S. Tong, Neural-network-based adaptive constrained control for switched systems under state-dependent switching law, *IEEE Trans. Neural Networks Learn. Syst.*, **34**(8):4057–4067, 2023, https://doi.org/10.1109/TNNLS.2021.3120999.

18. N. Tariq, I. Petrunin, S. Al-Rubaye, Analysis of synchronization in distributed avionics systems based on time-triggered ethernet, in *2021 IEEE/AIAA 40th Digital Avionics Systems Conference (DASC)*, IEEE, Piscataway, NJ, 2021, pp. 1–8, https://doi.org/10.1109/DASC52595.2021.9594327.

19. F. Wang, K. Chen, S. Zhen, X. Chen, H. Zheng, Z. Wang, Prescribed performance adaptive robust control for robotic manipulators with fuzzy uncertainty, *IEEE Trans. Fuzzy Syst.*, **32**(3):1318–1330, 2024, https://doi.org/10.1109/TFUZZ.2023.3323090.

20. T. Wang, G. Zong, X. Zhao, N. Xu, Data-driven-based sliding-mode dynamic event-triggered control of unknown nonlinear systems via reinforcement learning, *Neurocomputing*, **601**:128176, 2024, https://doi.org/10.1016/j.neucom.2024.128176.

21. L. Xiaofeng, A synchronization method for the avionic system interconnected by the local communication network, in *2022 IEEE 10th Joint International Information Technology and Artificial Intelligence Conference (ITAIC), Vol. 10*, IEEE, Piscataway, NJ, 2022, pp. 1020–1023, https://doi.org/10.1109/ITAIC54216.2022.9836642.

22. R. Yang, Y. Yu, Event-triggered control of discrete-time 2-D switched Fornasini–Marchesini systems, *Eur. J. Control*, **48**:42–51, 2019, https://doi.org/10.1016/j.ejcon.2018.12.008.

23. R. Yang, W.X. Zheng, Y. Yu, Event-triggered sliding mode control of discrete-time two-dimensional systems in roesser model, *Automatica*, **114**:108813, 2020, https://doi.org/10.1016/j.automatica.2020.108813.

24. X. Yang, X. Wan, C. Zunshui, J. Cao, Y. Liu, L. Rutkowski, Synchronization of switched discrete-time neural networks via quantized output control with actuator fault, *IEEE Trans. Neural Networks Learn. Syst.*, **32**(9):4191–4201, 2021, https://doi.org/10.1109/TNNLS.2020.3017171.

25. D. Yao, H. Li, Y. Shi, Event-based average consensus of disturbed MASs via fully distributed sliding mode control, *IEEE Trans. Autom. Control*, **69**(3):2015–2022, 2024, https://doi.org/10.1109/TAC.2023.3317505.

26. X. Zhang, J. Liu, X. Xu, S. Yu, H. Chen, Robust learning-based predictive control for discrete-time nonlinear systems with unknown dynamics and state constraints, *IEEE Trans. Syst. Man Cybern.: Syst.*, **52**(12):7314–7327, 2022, https://doi.org/10.1109/TSMC.2022.3146284.